Atmos. Meas. Tech. Discuss., 6, 8071–8105, 2013
www.atmos-meas-tech-discuss.net/6/8071/2013/
doi:10.5194/amtd-6-8071-2013

Atmospheric Measurement Techniques Discussions

Retrieval of characteristic parameters for water vapour transmittance in the development of ground based sun-sky radiometric measurements of columnar water vapour

M. Campanelli[1], T. Nakajima[2], P. Khatri[3], T. Takamura[3], A. Uchiyama[5], V. Estelles[4], G. L. Liberti[1], and V. Malvestuto[1,†]

[1]Consiglio Nazionale delle Ricerche (CNR), Institute of Atmospheric Science and Climate (ISAC), Rome, Italy
[2]Center for Climate System Research (CCSR), The University of Tokyo, Kashiwa, Japan
[3]Center for Environmental Remote Sensing(CEReS), Chiba University, Chiba, Japan
[4]Dept. Fisica de la Terra y Termodinamica, Facultat de Fisica, Burjassot, Valencia, Spain
[5]Meteorological Research Institute, Tsukuba-City, Japan
[†]died in May 2011

Received: 14 May 2013 – Accepted: 13 August 2013 – Published: 3 September 2013

Correspondence to: M. Campanelli (m.campanelli@isac.cnr.it)

Published by Copernicus Publications on behalf of the European Geosciences Union.

AMTD
6, 8071–8105, 2013

Abstract

Sun-sky radiometers are instruments created for aerosol study, but they can measure in the water vapour absorption band allowing the estimation of columnar water vapour in clear sky simultaneously with aerosol characteristics, with high temporal resolution. A new methodology, cheap and easy to implement, is presented for estimating calibration parameters (i.e. characteristic parameters of the atmospheric transmittance and solar calibration constant) directly from the sun-sky radiometers measurements. To initiate the proposed methodology some seasonal independent measurements of columnar water vapour taken over a large range of solar zenith angle simultaneously with the sun-sky radiometer measurements, are needed. In this work the Surface Humidity Method (SHM) was developed allowing to initiate the procedure with columnar water vapour estimated by standard surface meteorological observation (temperature, pressure and relative humidity). The time pattern of columnar water vapour from sun-sky radiometer was compared with simultaneous measurements from microwave radiometer and radiosondings showing respectively a total correlation of 0.98, 0.96 and a total median difference of 2.24 and −0.65 mm. The accordance with radiosondings was found within the uncertainty of the methodology (varying from 10 to 16 %) independently on the amount of atmospheric water vapour.

1 Introduction

Water vapour columnar content is an important parameter to be estimated since it is a greenhouse component affecting the Earth climate. Many techniques were developed for measuring the water vapour amount from satellite remote sensing, in the visible, infrared or microwave spectral regions, from ground based remote sensing, i.e. GPS, sunphotometers, microwave radiometers, or from radiosondings. Sun-sky radiometers are instruments designed for the aerosol study, and many of them can also measure in the water vapour absorption band, allowing estimation of the columnar water vapour

AMTD
6, 8071–8105, 2013

in clear sky condition, simultaneously with aerosol characteristics, with high temporal resolution up to few minutes. Despite the limits of sunphotometry technique related to clear sky daytime conditions, the high temporal sampling and the wide distribution of these instruments all over the world make the development of methodologies for retrieving columnar water from sun-sky radiometers of great interest. The most important problem in using these instruments is the estimation of the solar calibration constant and of the *a* and *b* parameters characterizing the atmospheric transmittance in the water vapour band, $T = e^{-a \cdot (m \cdot W)^b}$ (Bruegge et al., 1992), where *m* is the optical air-mass and *W* is the columnar water vapour content. Some methods for estimation of *W* from sun-sky radiometers have been already developed (Halthore et al., 1997; Alexandrov et al., 2009; Schmid et al., 2001). They are mainly based on the combined use of a radiative transfer code to determine the *a* and *b* parameters and of the Langley plot techniques for estimation of the solar calibration constant. Within the AERONET sun-sky radiometers network (Holben et al., 1998) a methodology for estimating *W* from the solar irradiance measured at wavelength of 940 nm has already implemented. Their algorithm is based on a use of a radiative transfer code (Smirnov et al., 2004) for computing *T* as a function of *W* and then estimating *a* and *b* parameters from a curve-fitting procedure. The solar calibration constant is determined by a modified Langley plot calibration performed at Mauna Loa Observatory (3400 m a.s.l). The uncertainty on its retrieval was found to be 10 times greater than the other wavelengths in the visible region, varying from 3 to 5 % (T. Eck, personal communication, 2009). A problem connected with these methodologies is that only one pair of (*a*, *b*) parameters is used for each kind of 940 nm interference filter, neglecting the dependence of *T* on the vertical profile of temperature, pressure and moisture at the various sites. This method is convenient for a network consisting of several instruments, but its correctness needs more investigations.

Campanelli et al. (2010) presented a new methodology for estimating *a* and *b* parameters directly from the measurements themselves, not relying on any radiative transfer calculation and therefore reducing simulation errors and potentially containing informa-

AMTD
6, 8071–8105, 2013

tion on seasonal changes in vertical profiles of temperature, air pressure, and moisture occurring at each measurement site. To initiate the proposed methodology some seasonal independent measurements of W (such those by radiosondes, microwave radiometers or GPS receivers) taken over a large range of solar zenith angle simultaneously with the sun-sky radiometer measurements are needed. In the previous paper, data of radiosondes were used for initializing the procedure but it was also considered when such independent measurements are not available. In the latter cases, the Surface Humidity Method (SHM) was developed allowing to initiate the procedure with W estimated by only measurements of surface temperature, pressure and relative humidity.

In the present paper we will examine in detail the accuracy and problems of the Surface Humidity Method, elaborating some points left opened in the previous paper: the study of a, b variation as a function of columnar water vapor amount; the estimation of a and b retrieval errors; the application of the methodology to an entire year dataset. Results will be compared against measurements taken by a microwave radiometer and radiosondes.

2 Equipment

The present methodology was applied to measurements performed during 2007 at the Chiba University (140.124° E 35.622° N, 34 km SE from Tokyo, Fig. 1) by the Center for Environmental Remote Sensing, Chiba University, Japan. A PREDE sun-sky radiometer model POM 02, part of Skynet network (Takamura and Nakajima, 2004; http://atmos.cr.chiba-u.ac.jp/), was used. This instrument is a scanning spectral radiometer taking measurements of solar direct and diffuse irradiance every 5 minutes at several wavelengths in the visible and near infrared regions appropriately chosen for aerosol study therefore clear from gas absorption. Measurements of direct solar irradiance taken at 940 nm are used for estimating the columnar water vapour content in clear sky conditions. Ancillary co-located measurements of pressure and relative hu-

AMTD
6, 8071–8105, 2013

midity, needed for the application of the Surface Humidity Method, were provided by the Japan Meteorological Agency.

Retrievals from the Sun-sky radiometer were compared against measurements taken from a microwave radiometer and from radiosondings. The former (co-located with the above mentioned instruments) is a Radiometrix WVR-1100 portable water vapour passive radiometer measuring microwaves radiation from the sky at 23.8 and 31.4 GHz. These two frequencies allow simultaneous determination of integrated liquid water and integrated vapour along a selected path. In the case of water vapour and liquid water, the atmosphere is rather translucent in the vicinity of the 22.2 Ghz water vapour resonance line, and total integrated water, water vapour and phase path delay can be derived thanks to their linear dependence on the atmospheric opacity at the measuring wavelengths. The coefficients of these linear equations are determined from bilinear regression of water vapour and inferred liquid water data derived from radiosonde observations.

Radiosonde measurements were extracted from the Integrated Global Radiosonde Archive (IGRA, http://www.ncdc.noaa.gov/oa/climate/igra/) that contains quality controlled radiosonde and pilot balloon observations at over 1500 globally distributed stations (Durre et al., 2006). The station closer to Chiba is Tateno (140.13° E, 36.05° N), in the prefecture of Ibaraki about 46 km N from Chiba. The information and sampling of the radiosondings contained in the IGRA archive are, in the majority of the cases, the ones originally sent to the Global Telecommunication System (GTS) of the World Meteorological Organization (WMO). The reported variables, in the IGRA dataset, are pressure [Pa], geopotential height [m], air temperature [°C], Dew Point Depression (DPD) [°C], wind direction [°] and speed [$m\,s^{-1}$]. Air temperature and DPD are reported with a 0.1 °C numerical discretization. Quality assurance flags are given, for each pressure, geopotential height, and temperature value, that indicates whether the corresponding value was checked by procedures based on climatological means and standard deviations. Concerning the vertical sampling in the reported profile, in accordance with WMO guidance, radiosondes should report: standard pressure levels (1000, 925, 850,

AMTD
6, 8071–8105, 2013

700, 500, 400, 300, 250, 200, 150, 100, 70, 50, and 10 hPa), surface, tropopause and significant thermodynamic and wind levels (WMO, 1986, 1995). Radiosonde estimates of the Total Precipitable Water Vapour are obtained by computing the specific humidity for each level, having valid: temperature, pressure and DPD measurements and then integrating numerically the specific humidity over the vertical using a pressure weighted numerical integration scheme.

3 Methodology

The direct solar irradiance measurement V [mA] taken by the sun-sky radiometer at the 940 nm wavelength in clear sky condition is related to the solar calibration constant V_0 (extra-terrestrial current mA) at the same wavelength through the following expression,

$$V = V_0 \cdot e^{-m\cdot(\tau_a+\tau_R)\cdot} \cdot e^{-a\cdot(m\cdot W)^b}, \quad (1)$$

where (i) m is the relative optical air mass (Kasten and Young, 1989) function of the solar zenith angle; (ii) τ_a and τ_R are the aerosol extinction optical thicknesses and molecular Rayleigh-scattering at 940 nm, respectively; and (iii) $T = e^{-a\cdot(m\cdot W)^b}$ is the water vapour partial atmospheric transmittance at 940 nm as a function of m and W, with a and b constants (Bruegge et al., 1992). Once a and b have been determined, V_0 can be estimated, and W can subsequently be calculated.

Equation (1) can be also written in the form,

$$y = \ln V_0 - a \cdot x, \quad (2a)$$

$$\text{with } \begin{cases} y = \ln V + m \cdot (\tau_a + \tau_R) \\ x = (m \cdot W)^b \end{cases}. \quad (2b)$$

The aerosol optical thickness τ_a is estimated at wavelength $\lambda = 940$ nm, according to the well-known Ångström formula,

$$\tau_a(\lambda) = \beta \lambda^{-\alpha}, \quad (3)$$

AMTD
6, 8071–8105, 2013

where wavelength λ is measured in μm, α is the so-called Ångström exponent, and β is the atmospheric turbidity parameter. Parameters α and β are determined by the regression from Eq. (3) where the spectral series of τ_a are retrieved by the sun-sky radiometer measurements taken at the other visible and near infrared wavelengths 400, 500, 675, 870, and 1020 nm.

In order to find the most appropriate pair of values (a, b), the following steps are followed: (i) x values are calculated for 30 different values of b from 0.4 to 0.7 with a step of 0.01 and each time the (x, y) squared correlation coefficient is calculated; then the maximization of the (x, y) squared correlation coefficient is used to determine the best exponent b; (ii) once the optimal b exponent is retrieved, the series of x values is computed and the coefficient a and V_0 can be found from Eq. (2a) by determining the regression line of y vs. x. This modified version of Langley plot (called "type-2 modified Langley") is different from the other modified Langley method described by Halthore et al. (1997) and Schmid et al. (2001) (called " type-1 modified Langley"). In fact whereas the latter determines V_0 as the intercept of the straight line obtained by fitting y versus the power term m^b, in the former V_0 is retrieved by plotting y versus the product $a \cdot x$ where $x = (m \cdot W)^b$. This approach largely improves the application of the Langley methods to cases where the time patterns of W is not stable. In fact the "type-1 modified Langley" assumes that y only depends on airmass, m, and that all points have the same W. When a variability of W is recorded, the neglected dependence of y on W causes a scatter of the points and introduces calibration errors and large day-to-day changes in the retrieved calibration constants. Conversely "type-2 modified Langley" gives evidence to the dependence of y on $(m \cdot W)$ and the variability of y is explained by the real variability of the product $(m \cdot W)$, providing a better retrieval of the intercept ($\ln V_0$) also when the time pattern of precipitable water content is not stable. In Fig. 2 type-1 and type-2 Langley plot methods were used to retrieve V_0 in two cases: stable (13 June 2007) and unstable (12 June 2007) time patterns of W as measured at Chiba by the microwave radiometer simultaneously to the sun-sky radiometer. It is clear that using type-2 method, the points are less scattered especially in the case

AMTD
6, 8071–8105, 2013

of more unstable W time pattern. In Table 1 the retrieved V_0 values are shown. The absolute difference between the V_0 values retrieved by the two methods from 12 to 13 June is only 1.8 % if type-2 is used, whereas increases up to 4.1 % when type-1 is adopted, highlighting the better capability of type-2 in estimating V_0 during both stable and unstable W time periods.

Once parameters V_0, a and b have been determined, the values of precipitable water content W_P, can be calculated according to the equation:

$$W_P = \frac{1}{m} \cdot \left[\frac{1}{a} \cdot (\ln V_0 - y) \right]^{\frac{1}{b}}. \quad (4)$$

With respect to the previous version published in Campanelli et al. (2010), the procedure was improved in two important aspects: the use of a Monte Carlo method for the evaluation of errors affecting the a and b values, and the application of the methodology to an entire year dataset. Concerning the first aspect the improvement consists in:

1. A pre-selection of dataset, (as described in Sect. 4) performed before the application of the methodology.
2. After the optimal values of a and b are found, the residual standard deviation $\sigma_{RES}$is computed around the optimal regression line.
3. A Monte Carlo approach is used to simulate 80 fictitious bivariate samples of the pair of variables $x_1 = m \cdot W$ and y, each fictitious sample sharing with the true sample:
   - the number N of data available
   - the lower and upper bounds of x_1
   - the noise around the ideal straight line.

AMTD
6, 8071–8105, 2013

More precisely, the x_1-data are generated by sorting N random values uniformly distributed between x_{1MIN} and x_{1MAX}, while the y data are generated by the formula: $y = \ln V_0 - a \cdot x_1^b + \text{noise}$, where the a and b (and then $\ln(V_0)$) values are the optimal values retrieved above for the given real sample, while the noise is a Gaussian noise with standard deviation coincident with σ_{RES}. Then for each of the 80 fictitious samples a search of the optimal a and b values is carried out using the same procedure followed to find the actual optimal values (i.e. by maximizing the determination coefficient R^2 of the regression line) . In this way, a list of 80 pairs (a, b) are retrieved. For each of these parameters it is then possible to evaluate both the mean and the standard deviation. The coincidence of the two means $\overline{a}$ and $\overline{b}$ with their respective ideal values is a test for the goodness of the optimization procedure. This coincidence has been successfully verified in all our Monte Carlo simulations. Given that, the standard deviation appears to be the best estimate of the standard error to associate to each of the actual optimal values a_{opt}, b_{opt}, and an improvement respect to the estimation obtained using a simple propagation error formula.

4. Optimal V_0 is calculated by the linear fit of Eq. (2a) using the pair a_{opt}, b_{opt}. The error affecting V_0 is obtained by evaluating the standard error on the regression line intercept ($\ln(V_0)$) and then applying a simple propagation error formula.

For what concerns the second improvement, the application of the methodology to an entire year dataset brought to the consideration that because a, b are supposed to depend on vertical profiles of temperature, air pressure, and moisture it is not correct to estimate their values "seasonally", since seasons are only a rough subdivision of the year, marked by changes in weather, measurement environment, and hours of daylight. Therefore we grouped the available independent W measurements (needed for initiating the procedure) in water vapor classes and a, b were provided for each class. Number of classes adopted in this study and their thresholds will be described in Sect. 4.

AMTD
6, 8071–8105, 2013

As already stated, when independent measurements of W taken over a large range of solar zenith angle are not available, the Surface Humidity Method (SHM) can be used. It consists in estimating W dataset using surface-level observations of moisture parameters that are much more common than those performed with radiosondes or microwave radiometers. According to Hay (1970) there is a linear dependence between precipitable water content (W_{SHM}) and water vapour partial pressure e_0 [hPa] at the surface, expressed by Eq. (5)

$$W_{SHM} = c_1 \cdot e_0 + c_2, \quad (5)$$

where the quantity e_0 is calculated as the product of surface relative humidity f_0 by the saturation water vapour pressure $E(T_0)$ [hPa], calculated as a function of surface temperature T_0 [K] according to Lowtran code formula (Kneizys et al., 1983). Estimation of coefficients c_1 and c_2 can be found in the literature, from different daily or monthly data-sets and from varying numbers of measurements and sites (for example Hay, 1970; Tuller, 1977; Choudhury, 1996; Liu, 1986).

4 Parameters estimation

With the aim of finding the initiating W dataset for Chiba site, the following considerations were done: in Tateno station only one radiosonde launch is performed during daytime and therefore this dataset can't be used for initiating the procedure; Chiba is equipped of both a sun-sky radiometer and a microwave radiometer, but usually it is not very common finding microwave radiometers in measurement sites. Therefore it was decided to use the SHM for initializing the process and then comparing water vapour obtained by PREDE sun-sky radiometer by means of Eq. (4) (W_P) against measurements taken by both the microwave radiometer (W_{MWR}) and radiosondes (W_{RDS}).

W_{SHM}, as defined in Eq. (5), was estimated using c_1 and c_2 coefficients taken from Yamamoto et al. (1971). They retrieved an empirical formula for the relation between

AMTD
6, 8071–8105, 2013

W_{SHM} and e_0 (Eq. 6) using aerological measurements taken between 1950–1970 at several Japanese stations, during clear sky conditions

$$W_{SHM} = \begin{cases} 0.14 \cdot e_0, & \text{for } e_0 \leq 15\,\text{hPa} \\ 0.18 \cdot e_0 - 0.60, & \text{for } 15 < e_0 \leq 25\,\text{hPa} \\ 0.23 \cdot e_0 - 1.85, & \text{for } e_0 > 25\,\text{hPa} \end{cases}. \quad (6)$$

The SHM is able to provide reliable estimation of precipitable water content when vertical humidity generally decreases as a function of height in a nearly exponential profile, but this assumption is not always verified. Figure 3 compares the monthly averages values of W_{SHM} and W_{MWR}. It is apparent that Ws_{HM} generally overestimates the microwave radiometer measurement, being most of the time within the standard deviation.

Undoubtedly an error in W_{SHM} estimation can affect the validity of Eqs. (2), but the precipitable water content amount by sun-photometric observations (W_P) can be derived accurately through Eq. (4), unless *a* and *b* coefficients are too far from reality, as it will be discussed in Sect. 6.

Simultaneous measurements of sun-sky radiometer *V* and W_{SHM} were selected for the application of Eqs. (2a) and (2b). All the estimations of W_{SHM} within 15 min before and after measurements of signal *V* were taken, and all the values of τ_A and τ_R within the same intervals were selected and averaged over 30-min time-intervals. The present method was applied in the range of solar elevation angle yielding $m < 8$.

A preliminary check on the quality of each dataset was performed as follows:

1. Data corresponding to τ_a (940 nm) > 0.4 are rejected.
   In the present study the cloud screening is performed by selecting only measurements whose RMS deviation between measured and reconstructed diffuse sky irradiance, in the wavelengths devoted to aerosol study, is lower than 8 %. This criterion assured the rejection of cloud-contaminated direct and diffuse irradiance measurements, but it could not exclude the contamination of high and thin cirrus clouds. Being the maximum average value of τ_a (500 nm) about 0.6, it is likely

AMTD
6, 8071–8105, 2013

that data having τ_a (940 nm) > 0.4 are contaminated by clouds, and for this reason they must be rejected.

2. Data taken before 13:00 LT (local time) from October to May were rejected. During these months the behaviour of y vs. x appears very often not linear, as shown in Fig. 4. In these cases two separate behaviours can be recognized generally one in the morning and one in the afternoon. This is likely related to the fact that in these months, conversely to summer season, more time is needed to break the stable conditions characterizing the low atmosphere after the nocturnal cooling period, and to let the vertical distribution of water vapour mass concentration develop in an exponential profile. For these months we decided, as first approximation, to select only measurements initiating from 13:00 LT in order to reduce the problem to a linear behaviour.

3. A statistical selection was applied to discard outliers with deviation greater than 2σ from the regression line.

Because a and b are supposed to depend on the vertical distribution of the columnar water vapour and then on its total amount: (i) the entire yearly W_{SHM} dataset was divided in four classes: [0–10]; [10–20]; [20–40]; [> 40] mm; an overlap between classes of ±1 mm has been considered for the thresholds of each class; (ii) the procedure was applied for each class with the aim of providing water vapour dependent a and b.

The choice of a larger interval for the third class is strictly related to the need of having a greater number of dataset. In fact as stated in Campanelli et al. (2010) a problem connected with the use of SHM is the need of a greater data-set of m W in order to reduce the effects originated by those cases where a clear linearity between y vs. x is not identified.

In Table 2 the number of points passing after the quality checks for each water vapour class is shown. In Fig. 5 plots of the type-2 modified Langley for each of the four water vapour classes are shown. Optimal values of (a, b) and V_0 for each WV class are shown in Table 2 and Fig. 6. The slightly dependence of V_0 on the water vapour class

AMTD
6, 8071–8105, 2013

is obviously a fictitious tendency introduced by the methodology; nevertheless its total uncertainty (estimated as the standard deviation of the values divided to their mean) resulted to be about 7 %, that is slightly largest than the maximum uncertainty retrieved by AERONET at Mauna Loa Observatory (5 %).

5 Water vapour estimation

Once the optimal parameters (a, b) and V_0 are estimated for each of the selected water vapour classes (four in the present study), a calibration table proper of the site and of the instrument under study, is made available. W_P can be instantaneously calculated as in Eq. (4) using this table, as soon as V (940 nm) and τ_a (940 nm) measurements are performed. To retrieve the water vapour content, an iterative procedure has been set up as follows: (i) for each V (940 nm) and τ_a (940 nm) measurement, W_P is calculated using the four set of parameters; (ii) each of the four W_P values falls in one class of water vapour: when at least three of them converge within the same class, the pertinent parameters to be used for the current measurement are identified. The W_P values were calculated for 2007 and compared against measurements taken by the Microwave Radiometer (W_{MWR}) and Radiosondings (W_{RDS}) selecting simultaneous measurements within ±15 min and ±1 h, respectively. It must be taken into account that only W_{RDS} measurements taken at 09:00 LT can be compared with W_P estimations. The percentage uncertainty of W_P ($\Delta W_P / W_P$), calculated as maximum error, was estimated by means of propagation error formulas, considering that the quantities affected by errors in Eq. (4) are V_0, τ_A, a, and b (Table 2). The uncertainty $\Delta\tau_A$ was calculated by means of propagation error formulas of Eq. (3). Scatter plots of W_P versus W_{MWR} and W_{RDS} are shown in Fig. 7a and b, corresponding correlation coefficients and median differences are indicated in Table 3. The W_P was found to be very well correlated with both W_{MWR} and W_{RDS} (total correlation respectively 0.98, 0.96) and the median difference showed a general overestimation of W_P respect to W_{MWR} (2.24 mm) and an underestimation respect to W_{RDS} (−0.65 mm). For each class the median percentage difference

AMTD
6, 8071–8105, 2013

with W_{RDS} was always within the uncertainty $\Delta W_P / W_P$, whereas the median percentage difference with microwave radiometer for low content of columnar water vapor (first class, 85 %) strongly exceeded the threshold. In this case the agreement strongly decreased also in correlation (0.58), showing a significant underestimation of water vapor abundance measured by the microwave radiometer. The similar kind of disagreement was recognizable also when W_{MWR} was compared against W_{RDS} (Fig. 7c), likely due to a pure accuracy of the inversion algorithm of the microwave radiometer for very low water vapour content. On the other hand larger disagreement between W_P and W_{RDS} was visible for the class [20–40] mm, mostly due to the presence of several points where water vapour is strongly underestimated by the sun-sky radiometer (Fig. 7b). In Fig. 8 the vertical profile of water vapour mixing ratio as measured by the radiosonde is plotted in black for the two days showing the maximum disagreement (7 and 9 August) and in grey for two days where their difference is lower than 2 % (16 and 22 August). From the comparison it is highlighted that the black curves indicate the presence of a thick layer of water vapour from the ground up to about 800 hPa, whereas the grey ones are close to an exponential behaviour. Since the formulation of W_{SHM} in Eq. (6) assumes the vertical profile of water vapour as an exponentially decreasing curve with a prescribed height scale, it is reasonable to have an underestimation of the real water vapour abundance due to a sort of smoothing of the real stratifications.

In order to validate and verify the possible improvements taken by the proposed methodology, a simulation of the transmittance was performed using a radiative transfer code written by A. Uchiyama. In particular the filter response function of the PREDE POM 02 was sampled; six original atmospheric models from McClatchey's (1972) (tropical, mid latitude summer, mid latitude winter, subarctic summer, subarctic winter, US standard atmosphere 1962) and four modified profiles obtained by reducing the column water vapour of one tenth, were used to calculate the transmittance at 10 different hours in order to simulate a large range of path length. 100 pairs of mW and simulated transmittance ($T = e^{-a \cdot (m \cdot W)^b}$) were obtained and used to calculate by a fitting procedure the following parameters: $a_s = 0.141$, $b_s = 0.626$. V_0 was

AMTD
6, 8071–8105, 2013

calculated using the Type-2 modified Langley applied to five days having a smoothed water vapour diurnal time pattern and daily average values covering the range between 5 to 35 mm. Their mean value and standard deviation was performed to calculate $V_{0s} = 2.33 \times 10^{-4}$ (mA) with an uncertainty of 3.5 %. a_s, b_s and the mean V_{0s} value resulted to be comparable with values provided by the SHM methodology in the class having the highest water vapour content (Fig. 6). a_s, b_s and V_{0s} were therefore used in Eq. (4) to estimate the columnar water vapour W_s. The scatter plot of W_S versus W_P (Fig. 7d) showed a good agreement between the two water vapor estimations that are always within the ΔW_P uncertainty even if an underestimation of W_P is recognizable for the class [20–40] mm. W_S was also compared against W_{MWR} and W_{RDS} (Table 3) showing correlation and median difference, both total and for each class, comparable with the one provided by the SHM methodology. Conversely the accordance between W_S and the Microwave Radiometer get worse in median difference for all the classes, with the exception of the fourth one [> 40] mm.

In conclusion the columnar water vapour calculated by simulation of atmospheric transmittance was found to be comparable with the retrievals by the SHM methodology, being always within the uncertainty $\Delta W_P / W_P$, but we like to emphasize that the introduction of a water vapor dependence in *a* and *b* parameters improved the agreement with the Microwave Radiometer measurements especially for the lowest water vapour content. The accordance between W_P and W_{RDS} was always found within the uncertainty $\Delta W_P / W_P$.

This important outcome validates the goodness of the SHM method and leads to the conclusion that simultaneous use of the simulation method and SHM method can improve the water vapour product from the sun-sky radiometers, because of the capability of the SHM method of monitoring the time change of *a* and *b* values on each site and then monitoring the instrumental condition.

AMTD
6, 8071–8105, 2013

6 Discussion

Looking at the water vapour dependence of the a, b and V_0 parameters in Fig. 6, two aspects are particularly noticeable. The first one is that their behaviours are somehow connected since the increase of one parameter is balanced by the decrease of another. This is due to the fact that in the applied methodology of maximization these variables are not calculated independently one from the other. It implies that, at the present stage, the retrieved V_0 should be considered as an effective calibration constant and therefore its temporal variation could not be related to a real instrumental drift.

The second aspect is that the b value for class [0–10] (and therefore also a, and V_0) seems to be too different (in particular too low) respect to the ones retrieved with the SHM for the other classes and to that estimated by the fitting procedure of simulated transmittance (Fig. 6). Nevertheless W_P and W_S for this class are in good agreement as it is shown in Fig. 7d, with a median difference of 11%. To explain this effect, a study of the Jacobian elements from the derivative of Eq. (4) for the coefficients a and b has been performed. The analysis showed that the Jacobian for the a coefficient is approximately 3 times the one for the b coefficient, being both negative. Therefore any sets of a and b coefficients can introduce the same error in W_P determination, if the difference between b values is up to −3 times the difference between a values. When this rule is respected, two pairs of a and b can provide exactly the same W_P. In our case the difference between optimal b value and b_s is −1.5 times the difference between a and a_s, and this explains the good accordance between W_P and W_S.

This analysis takes to the conclusion that there is a non-unique solution in the application of the SHM, unless we identify which vertical profiles of water vapour are able to provide such low b values during winter time. The problem is likely linked to the non linearity of y vs. x during this season, and needs to be investigated in a next future through simulations studies.

The application of the Surface Humidity Method needs the determination of the coefficients explaining the linearity between precipitable water content and water vapour

AMTD
6, 8071–8105, 2013

partial pressure. In the case under study we used an empirical formula for the relation between W and e_0 obtained from a climatologic study typical of Japan, but this kind of study could not be always available for every site. One solution to this problem could be determining the proper coefficients in Eq. (6) by using already existing historical datasets of W and e_0 measured in proximity of the site under study. If this is neither possible, estimation of coefficients c_1 and c_2 can be found in the literature, from different daily or monthly data-sets and from varying numbers of measurements and sites. With the aim of checking the error introduced if not appropriate coefficients are used for the estimation of W_{SHM}, the Choudhury (1996) formulation was considered. Choudhury examined a data set consisting of monthly mean values of W and e_0 taken at 45 stations distributed over the entire planet, obtaining the average global values $c_1 = 1.70$ and $c_2 = -0.1$. The stations were far from water surfaces, with negligible influences due to evaporation and transport of humid air from marine regions, that are conditions not respected at all in the site under examination. Ws_{HM} calculated by Choudhury formulation, was used in Eqs. (2a) and (2b) for estimating the best a, b and V_0 in each water vapour class, and water vapour from the Sun-sky radiometer (W_{PC}, where the subscript c stands for discrimination from the W_P retrieved using Yamamoto formulation) was calculated using Eq. (4). Linear fitting of the scatter plot between W_P and W_{PC} (Fig. 9a) shows an intercept value of -1.22 and a slope value of 0.92. This result indicates that even though the application of the Surface Humidity Method can affect the validity of Eqs. (2) when completely not appropriate parameters are used for estimating W_{SHM}, this inaccuracy introduces an error mostly consisting of a bias, positive in our case. This is also confirmed by the scatter plot of the (normalized) time derivatives of the W_P and W_{PC} time series ($\frac{\Delta W_P}{\Delta t}$ and $\frac{\Delta W_{PC}}{\Delta t}$) in Fig. 9b). In fact the optimum agreement between the two series shows that W_P and W_{PC} have the same temporal behaviour.

This means that in the case when the absolute calibration (in terms of a, b, V_0) is not correct, information from the relative values of W_{PC} and its time derivatives can be extremely valuable, being the temporal resolution of measurements high (generally

AMTD
6, 8071–8105, 2013

between 5 to 10 min). However it is strongly suggested to not use formulas of linearity between W and e_0 obtained for sites with characteristics completely different from the place under study.

In order to have available the calibration table proper of the site and the instrument under study, showing the water vapour dependence of the optimal parameters a, b and V_0, a new user installing a sun-sky radiometer for the first time must wait to built a statistically significant dataset for the fit, before having columnar water vapour estimations. This time is needed to collect simultaneous measurement of direct solar irradiance and pressure, temperature and relative humidity (in the case when SHM method is used) or other independent measurements provided that they cover the entire range of variability of columnar water vapour typical of the site under study. This gap could be filled at the beginning of operations by using the method based on the simulation of transmittance, with the intent of the reprocessing data once the calibration table is available.

An innovative application of the presented procedure could be the possibility of providing an estimation of water vapour scale height using W_P and the water vapour obtained at the ground from pressure temperature and relative humidity measurements, provided for example from the installation of sensors on the head of the PREDE sun-sky radiometer. In fact

$$W_P = C \int W_0 \cdot e^{-\frac{z}{z_0}} \mathrm{d}z \tag{7}$$

where W_0 is the water vapour density at the Earth's surface , z_0 is the scale height (km) and C is a constant taking into account the unit of measurements conversion. By inverting Eq. (7) it is possible to determine z_0 and therefore providing a sort of vertical profile from an instrument that typical retrieves only columnar properties.

AMTD
6, 8071–8105, 2013

7 Conclusions

A procedure, cheap and easy to implement for determining columnar water vapour from Sun-sky radiometers measurements of direct solar irradiance at 940 nm has been introduced. To initiate the methodology some seasonal independent measurements of water vapour taken over a large range of solar zenith angle simultaneously with the sun-sky radiometer measurements, are needed. In the present paper the procedure was initiated using the Surface Humidity Method developed using measurements of surface temperature, pressure and relative humidity. The goodness and weakness of the Surface Humidity Method was examined developing some points left opened in the previous paper Campanelli et al. (2010): the study of a, b variation as a function of columnar water vapour amount; the estimation of a and b retrieval errors; the application of the methodology to an entire year of dataset. The yearly time patter of W_P was compared against simultaneous measurements taken by a microwave radiometer and radiosondings showing a total correlation of 0.98, 0.96 and a median difference of 2.24 and −0.65 mm, respectively. The accordance with W_{RDS} was found within the uncertainty $\Delta W_P / W_P$ in all the four water vapour classes in which the dataset was divided, although few points in the class [20–40] mm showed a strong underestimation by W_P related to the presence of a thick water vapour layer that makes fail the assumption of an exponential vertical profile. The accordance against W_{MWR} strongly decreased for low content of columnar water vapour. However the same kind of disagreement was recognizable when W_{MWR} was compared against W_{RDS} probably due to a limitation of the inversion algorithm of the Microwave Radiometer for very low water vapour content.

Results were also validated against the columnar water vapour W_S estimated by using the most common procedure adopted for example by AERONET network, that consists in retrieving a and b parameters from a fitting procedure of simulated transmittance versus the product $m\,W$. Also in this case the accordance of W_S against W_{MWR} and W_{RDS} is good for all the water vapour classes, but we like to emphasize that the introduction of a water vapour dependence in a and b parameters improved the agree-

AMTD
6, 8071–8105, 2013

ment with the Microwave Radiometer measurements especially in the cases with the lowest water vapour content.

Although the problems connected to the application of the Surface Humidity Method (independency of the a, b and V_0 retrievals, determination of the coefficients explaining the linearity between W and e_0) absolute values of columnar water vapour from the Sun-sky radiometers were found in good agreement with the product from different instruments. In the case when the absolute calibration (in terms of a, b, V_0) resulted to be not correct, information from W_P relative values and time derivatives can be anyway extremely valuable.

In conclusion we retain that the simultaneous use of the simulation method and SHM method can be one solution to make the water vapour product from the sun-sky radiometer healthy, because the SHM method can monitor the instrumental condition through estimation of the time change of a and b values on each site. Moreover the advantage of having simultaneous measurements of aerosol characteristics and water vapour columnar content with a high temporal resolution and obtained by using only standard surface meteorological observation for calibrating the instrument, can be of great interest to the scientific community. The present procedure will be in the next future applied to the instruments that are part of SKYNET (Takamura and Nakajima, 2004; http://atmos.cr.chiba-u.ac.jp/) and ESR (Campanelli et al., 2012; http://www.euroskyrad.net/) networks in which web page the open source software will be released. It will also be tested on AERONET sun-sky radiometers in order to compare the two methodologies.

Acknowledgements. This work is dedicated to the memory of our colleague and friend Vincenzo Malvestuto. He was always curious to deal with all scientific aspects, with spontaneous and generous intellectual honesty, artistically creating mathematical and statistical methodologies for explaining measurements. He gave a fundamental contribution to this work developing with passion and enthusiasm the Monte Carlo approach. He passed away before this work was finished, leaving us with a deep sense of emptiness.

V. Estélles thanks the Spanish Ministry of Science and Innovation (MICINN) for the research contract under the Juan de la Cierva programme (JCI-2009-04455).

AMTD
6, 8071–8105, 2013

References

Alexandrov, M. D., Schmid, B., Turner, D. D., Cairns, B., Oinas, V., Lacis, A. A., Gutman, S. I., Westwater, E. R., Smirnov, A., and Eilers, J.: Columnar water vapour retrievals from multifilter rotating shadowband radiometer data, J. Geophys. Res., 114, D02306, doi:10.1029/2008JD010543, 2009.

Bruegge, C. J., Conel, J. E., Green, R. O., Margolis, J. S., Holm, R. G., and Toon, G.: Water 15 vapor column abundances retrievals during FIFE, J. Geophys. Res., 97, 18759–18768, 1992.

Campanelli, M., Lupi, A., Nakajima, T., Malvestuto, V., Tomasi, C., and Estelles, V.: Columnar content of atmospheric water vapour from ground-based sun/sky radiometer measurements through a new in-situ procedure, J. Geophys. Res., 115, D19304, doi:10.1029/2009JD013211, 2010.

Campanelli, M., Estelles, V., Smyth, T., Tomasi, C., Martìnez-Lozano, M. P., Claxton, B., Muller, P., Pappalardo, G., Pietruczuk, A., Shanklin, J., Colwell, S., Wrench, C., Lupi, A., Mazzola, M., Lanconelli, C., Vitale, V., Congeduti, F., Dionisi, D., and Cacciani, M.: Monitoring of Eyjafjallajoekull volcanic aerosol by the new European SkyRad users(ESR) sun-sky radiometer network, Atmos. Environ., 48 33–45, 2012.

Choudhury, B. J.: Comparison of two models relating precipitable water to surface humidity using globally distributed radiosonde data over land surfaces, Int. J. Climatol., 16, 663–675, 1996.

Durre, I., Vose, R. S., and Wuertz, D. B.: Overview of the Integrated Global Radiosonde Archive, J. Climate, 19, 53–68, 2006.

Halthore, R. N., Eck, T. F., Holben, B. N., and Markham, B. L.: Sun photometric measurements of atmospheric water vapor column abundance in the 940 nm band, J. Geophys. Res., 102, 4343–4352, doi:10.1029/96JD03247, 1997.

Hay, J. E.: Precipitable water over Canada: Part I. Computation, Atmosphere, 8, 128–143, 1970.

Holben, B. N., Eck, T. F., Slutsker, I., Tanre, D., Buis, J. P., Setzer, A., Vermote, E., Reagan, J. A., Kaufman, Y. J., Nakajima, T., Lavenu, F., Jankowiak, I., and Smirnov, A.: AERONET – A federated instrument network and data archive for aerosol characterization, Remote Sens. Environ., 66, 1–16, 1998.

AMTD
6, 8071–8105, 2013

Kasten, F. and Young, A. T.: Revised optical air mass tables and approximation formula, Appl. Optics, 28, 4735–4738, 1989.
Kneizys, F. X., Shettle, E. P., Gallery, W. O., Chetwynd, J. H., Abreu, L. W., Selby, J. E. A., Clough, S. A., and Fenn, R. W.: Atmospheric Transmittance/Radiance: Computer Code LOWTRAN 6, AFGL-TR-83-0187, Environmental Research Papers No. 846, Air Force Geophysics Laboratory, Hanscom Air Force Base, MA, 1983.
Liu, W. T.: Statistical relation between monthly mean precipitable water and surface level humidity over global oceans, Mon. Weather Rev., 114, 1591–1602, 1986.
McClatchey, R. A., Fenn, R. W., Selby, J. E. A., Volz, F. E., and Garing, J. S.: Optical Properties of the Atmo sphere, 3rd Edn., AFCRL 72-0497, AD 753075, L. G. Hanscom Field, Bedford, Massachusetts, 1972.
Schmid, B., Michalsky, J. J., Slater, D. W., Barnard, J. C., Halthore, R. N., Liljegren, J. C., Holben, B. N., Eck, T. F., Livingston, J. M., Russell, P. B., Ingold, T., and Slutsker, I.: Comparison of columnar water vapor measurements from solar transmittance methods, Appl. Opt., 40, 1886–1896, 2001.
Smirnov, A., Holben, B. N., Lyapustin, A., Slutsker, I., and Eck, T. F: AERONET processing algorithms refinement, paper presented at AERONET Workshop, AERONET, PHOTON, 10–14 May 2004, El Arenosillo, Spain, 2004.
Takamura, T. and Nakajima, T.: Overview of SKYNET and its activities, Opt. Pura Appl., 37, 3303–3308, 2004.
Tuller, S. E.: The relationship between precipitable water content and surface humidity in New Zealand, Arch. Meteorol. Geophys. Bioklimatol. Ser. A, 26, 197–212, 1977.
World Meteorological Organization: Algorithms for Automatic Aerological Soundings (A. H. Huper), Instruments and Observing Methods Report No. 21, WMO-TD-No. 175, Geneva, 1986.
World Meteorological Organization: Manual on Codes International Codes VOLUME I.1 Part A – Alphanumeric Codes, WMO–No. 306, Paragraph 35.3.1.3, Geneva, 1995.
Yamamoto, G., Tanaka, M., and Arao, K.: Secular variation of atmospheric turbidity over Japan, J. Meteorol. Soc. Jpn., 49, 859–865, 1971.

AMTD
6, 8071–8105, 2013

Table 1. Retrieval of V_0 for a stable and unstable water vapor time pattern cases, using type-1 and type-2 modified Langley methods.

V_0[mA]	12 June	13 June	% Diff.
type-1	2.17×10^{-4}	2.28×10^{-4}	4.1 %
type-2	2.23×10^{-4}	2.19×10^{-4}	−1.8 %

AMTD
6, 8071–8105, 2013

Table 2. Number of data points for each classes; optimal values of a, b and V_0 for each water vapor class and their estimated errors; estimated uncertainties of water vapor from sun-sky radiometer retrieved using the present methodology, W_P, and aerosol optical thickness, τ_A, for each of the four classes.

Classes (mm)	Number of points	a	b	$V_0 \times 10^{-4}$	Δa	Δb	$\Delta V_0 \times 10^{-4}$	$\Delta \tau_A$	ΔW_P %
[0–1]	601	0.218	0.52	2.49	0.002	0.02	0.02	0.0009	10.7
[10–20]	643	0.143	0.60	2.09	0.002	0.03	0.03	0.0022	16.0
[20–40]	977	0.166	0.60	2.39	0.002	0.02	0.04	0.0008	10.9
[> 40]	476	0.142	0.62	2.34	0.001	0.02	0.03	0.0023	9.8

AMTD
6, 8071–8105, 2013

Table 3. Correlation and median difference of retrievals from sun-sky radiometer using the present methodology (W_P) and the simulation of atmospheric transmittance (W_S) against measurements taken by Microwave Radiometer (W_{MWR}) and Radiosondings (W_{RDS}).

Classes (mm)	$R^2(N_{points})$		Median difference (mm; %)	
	W_P, W_{MWR} W_S, W_{MWR}	W_P, W_{RDS} Ws, W_{RDS}	$W_P - W_{MWR}$ Ws – W_{MWR}	$W_P - W_{RDS}$ Ws – W_{RDS}
[0–10]	0.58 (5955) 0.56 (5296)	0.69 (47) 0.66 (44)	3.36; 85 % 4.18; 123 %	−0.58; −8 % −0.09; 1 %
[10–20]	0.75 (5546) 0.86 (5925)	0.87 (20) 0.90 (23)	2.19; 18 % 3.38; 33 %	−0.25; −1 % −0.21; −2 %
[20–40]	0.91 (3838) 0.95 (4173)	0.85 (15) 0.86 (16)	0.36; 1 % 2.43; 8 %	−2.87; −9 % −0.37; −1 %
[> 40]	0.86 (1879) 0.83 (1931)	0.69 (8) 0.67 (9)	3.38; 7 % 1.78; 4 %	−0.11; −0.2 % −1.55; −3 %
All the classes	0.98 (14 919) 0.99 (14 919)	0.96 (79) 0.97 (79)	2.24 2.71	−0.65 −0.07

AMTD
6, 8071–8105, 2013

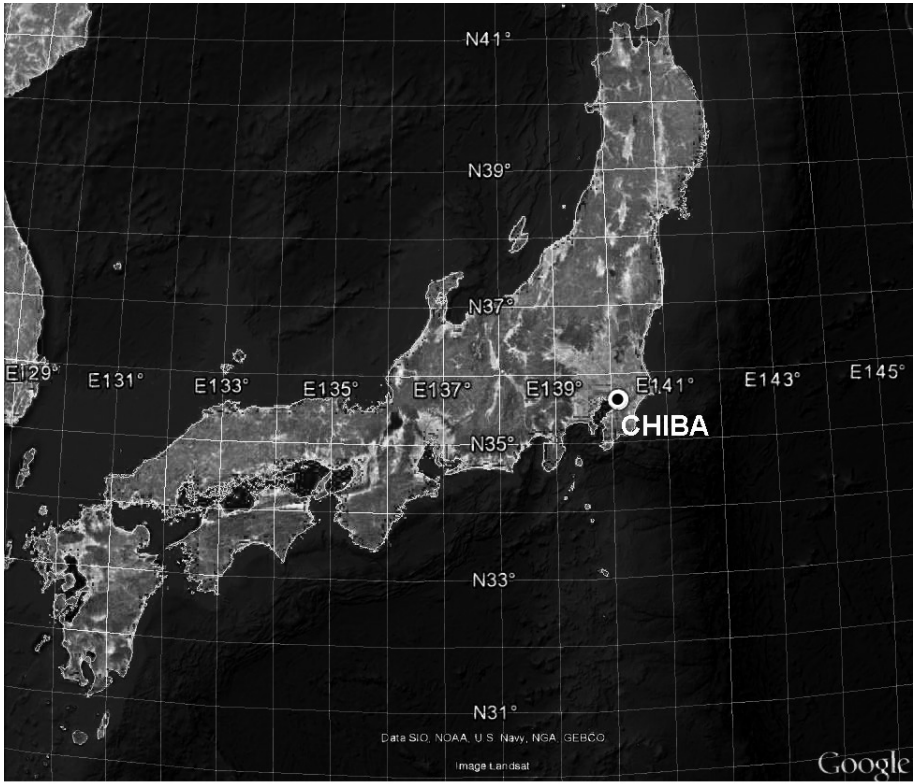

Fig. 1. Geographical position of the Chiba station in Japan.

AMTD
6, 8071–8105, 2013

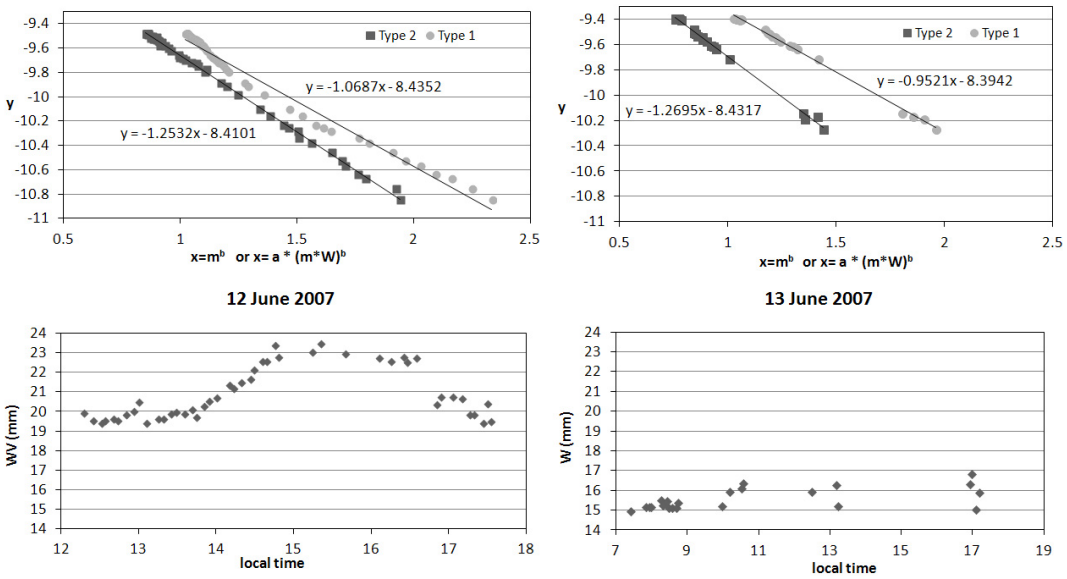

Fig. 2. Water vapour time pattern and application of type-1 and type-2 modified Langley methods for a stable (right panels) and unstable (left panels) water vapour time pattern cases. A fixed indicative value of $b = 0.6$ (as suggested by Halthore et al., 1997, for narrow band filters) has been assumed.

AMTD
6, 8071–8105, 2013

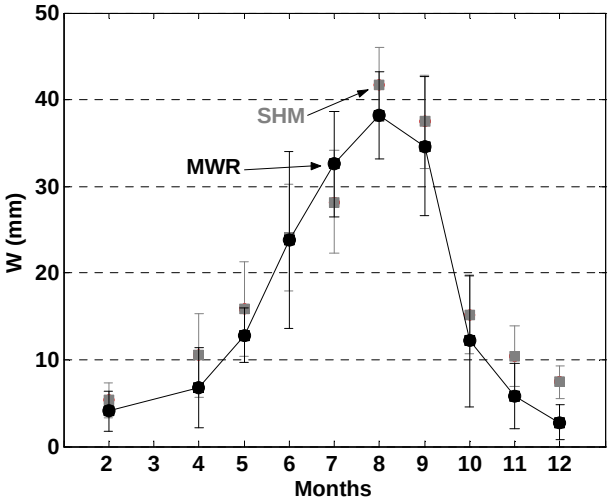

Fig. 3. Time pattern of the monthly average value of W_{MWR} and W_{SHM}. Error bars refer to the standard deviation.

AMTD
6, 8071–8105, 2013

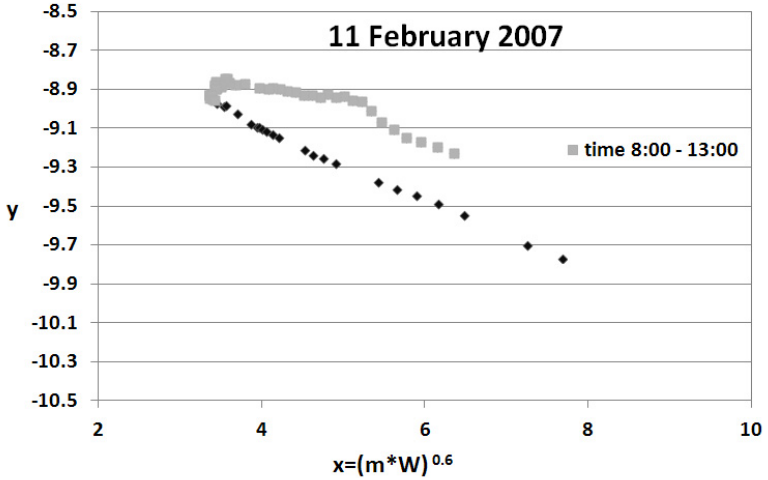

Fig. 4. *x* value calculated for a fixed indicative $b = 0.6$ (as suggested by Halthore et al., 1997, for narrow band filters).

AMTD
6, 8071–8105, 2013

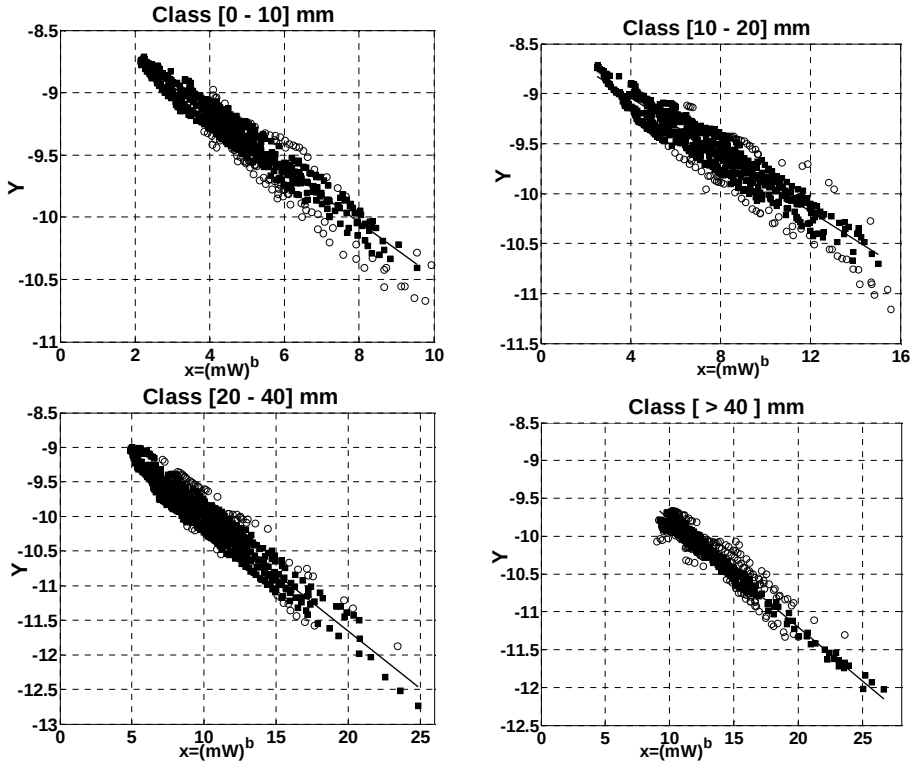

Fig. 5. Type-2 modified Langley for each of the four water vapour classes. Open circles are points discarded from the quality check selection. *b* is the retrieved optimal value for each class.

AMTD
6, 8071–8105, 2013

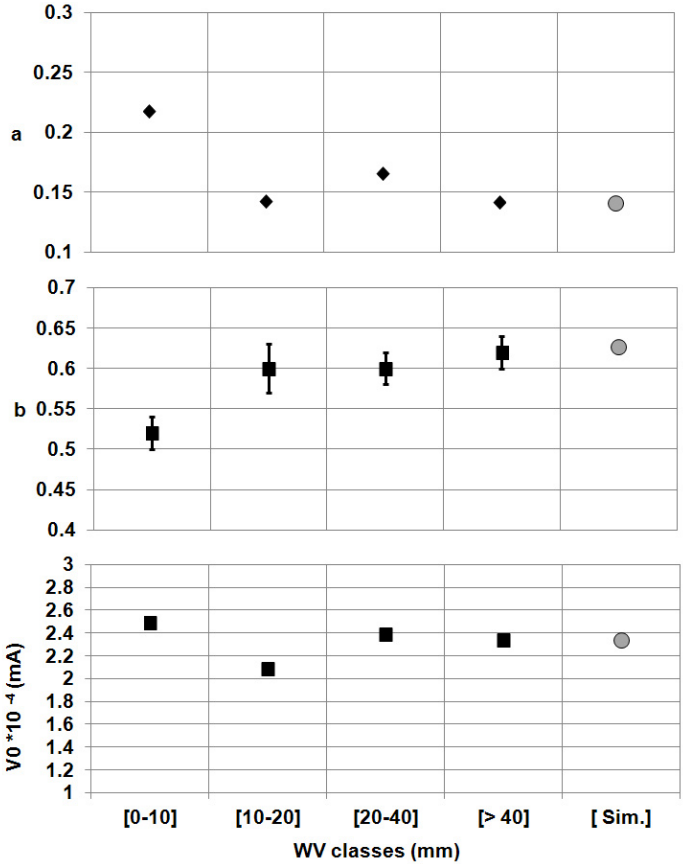

Fig. 6. Parameters *a*, *b* and V_0 as estimated by the presented methodology (black points). The grey point refers to the retrieval obtained by a fitting procedure of a simulated transmittance.

AMTD
6, 8071–8105, 2013

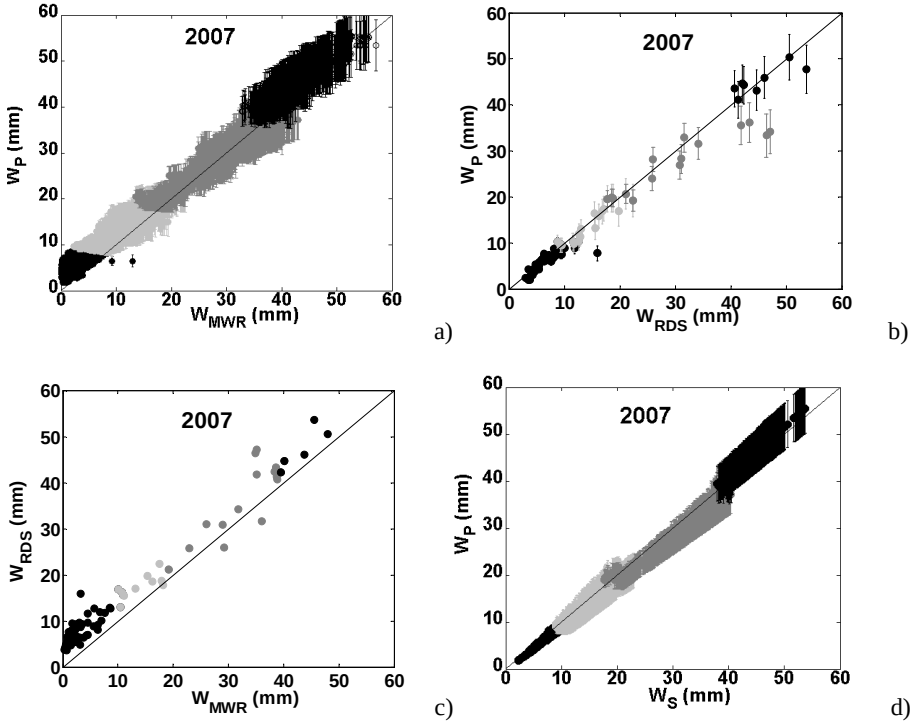

Fig. 7. Scatter plots of water vapour from sun-sky radiometer retrieved using the present methodology (W_P) versus measurements taken by Microwave Radiometer, W_{MWR} **(a)**, Radiosondings, W_{RDS} **(b)**, simulation of the atmospheric transmittance, W_S **(d)**, and of W_{RDS} versus W_{MWR} **(c)**. Alternation of greys and black colours indicate the four water vapour classes. Error bars for W_P correspond to the uncertainty retrieved for each class.

AMTD
6, 8071–8105, 2013

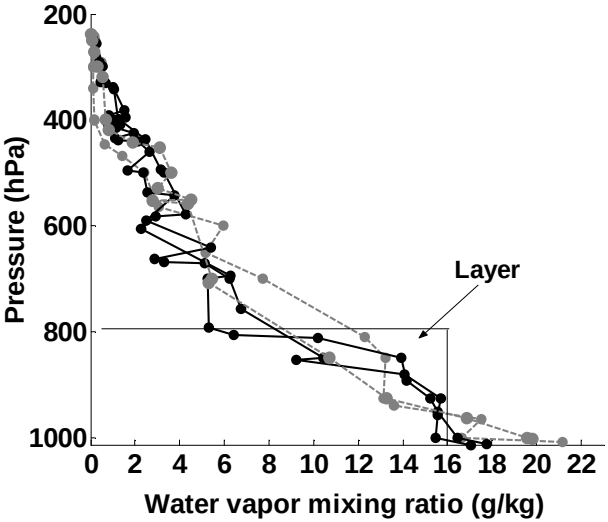

Fig. 8. Vertical profiles of water vapour mixing ratio as measured by the radiosonde. Black curves correspond to the profiles of days with maximum disagreement between W_P and W_{RDS} (7 and 9 August) due to the presence of a layer of water vapour; grey curves correspond to days with the difference lower than 2 % (16 and 22 August), when exponential vertical profile is recognisable.

AMTD
6, 8071–8105, 2013

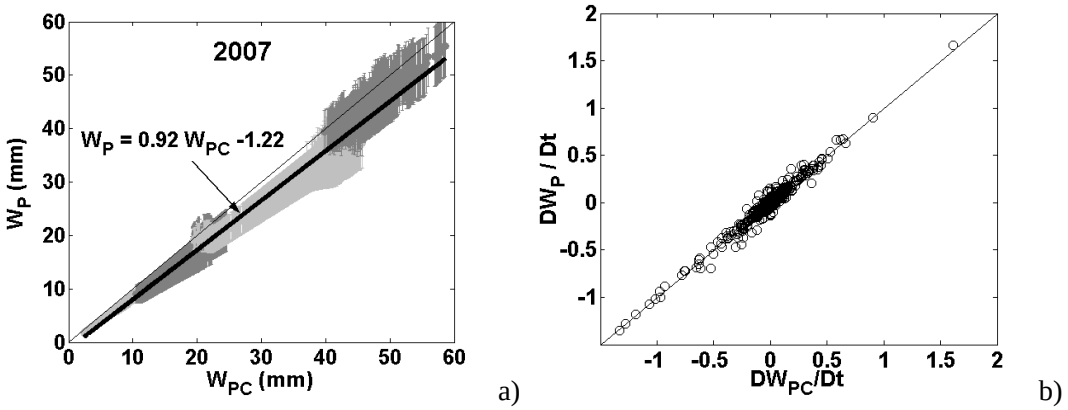

Fig. 9. Scatter plots of W_P versus water vapour obtained using the Choudhury formulation , W_{PC} **(a)** and their normalized time derivatives **(b)**.

AMTD
6, 8071–8105, 2013